Journal of Power Sources 196 (2011) 7973–7978

Contents lists available at ScienceDirect

Journal of Power Sources

journal homepage: www.elsevier.com/locate/jpowsour

Platinum nanoparticles supported on electrospinning-derived carbon fibrous mats by using formaldehyde vapor as reducer for methanol electrooxidation

Miaoyu Li, Yunzhen Chang, Gaoyi Han*, Binsheng Yang*

Institute of Molecular Science, Key Laboratory of Chemical Biology and Molecular Engineering of Education Ministry, Shanxi University, Taiyuan 030006, PR China

ARTICLE INFO

Article history:
Received 18 May 2011
Accepted 21 May 2011
Available online 27 May 2011

Keywords:
Electrospinning
Carbon nanofibers
Methanol
Pt nanoparticles
Formaldehyde vapor

ABSTRACT

The Pt nanoparticles have been well dispersed on electrospinning-derived carbon fibrous mats (CFMs) by using formaldehyde vapor as reducer to react with $H_2PtCl_6{\cdot}6H_2O$ adsorbed on the CFMs at 160 °C. The prepared electrodes of Pt-CFMs have been characterized by using scanning electron microscopy, transmission electron microscopy and X-ray diffraction spectroscopy, and the performance of the electrodes for methanol oxidation has been investigated by using cyclic voltammetry, chronoamperometry, quasi-steady state polarization and electrochemical impedance spectroscopy techniques. The results demonstrate that Pt-CFMs electrodes exhibit peak current density of 445 mA mg^{-1} Pt, exchange current of 235.7 μA cm^{-2}, charge transfer resistance of 16.1 Ω cm^2 and better stability during the process of methanol oxidation, which are superior to the peak current density of 194 mA mg^{-1} Pt, exchange current of 174.7 μA cm^{-2} and charge transfer resistance of 39.4 Ω cm^2 obtained for commercial Pt/C supported on CFMs. It indicates that the novel process in which formaldehyde vapor is used as reducer to prepare Pt catalyst with high performance can be developed.

1. Introduction

Many endeavors have focused on the development of energy conversion device with high efficiency in order to satisfy the needs of ever-increasing energy and tackle the environmental issues. Fuel cells are considered to be the energy conversion device with high efficiency because they convert the chemical energy into electric energy directly, among which, direct methanol fuel cells (DMFCs) have potential applications in low emission vehicles, portable electronic devices and distributed home power generators and attract enormous interest because of their high power density and low operating temperature [1–4]. The cathode and anode catalysts for oxygen reduction and methanol oxidation in DMFCs are usually Pt and its alloys due to their higher activity. However, the industrialization of DMFCs is still restricted by the high cost of the catalysts and the low activity and stability caused by the poisoning [4,5]. Thus, it is important to improve the activity and stability of Pt catalysts for methanol electrooxidation.

It has been proved that the performance of Pt catalysts for methanol electrooxidation depends not only on the size, shape and distribution of the particles but also on the categories and properties of the supporting materials [6–8]. Carbonaceous materials are currently being used as supports for Pt catalysts because of their high conductivity and multiformity of three-dimensional structures [9–13]. Nevertheless, it is a real challenge to develop high-quality carbon supports for catalysts with higher performance towards methanol electrooxidation although many such carbon materials as carbon black, carbon nanotubes, mesoporous carbon have been used as supports [4,9,13–16].

Recently, it is found that fibrous catalytic packs can be developed as an attractively alternative supporting material in DMFCs because of advantages such as short diffusion distance, fixation for catalysts, high conductivity and low resistance to flow of liquid and gas [12]. In the past years, electrospinning technique has been recognized as an efficient method to produce webs of nanofibers for applications in electrode, sensor and tissue engineering [17–23]. Conductive carbonaceous webs can be conveniently fabricated by a judicious combination of electrospinning and thermal treatment, and have been used as the electrode material in high-power supercapacitors and lithium-ion batteries [17–19]. The Pt particles deposited on the carbon fibrous mats (CFMs) can meet the requirements for reactant access, proton access and electronic continuity in DMFCs for the remarkable porous structure, close contact between the nanofibers and the high surface area of the electrospun fibrous mats.

In present work, the Pt particles supported on the CFMs are prepared by combining the process of physical adsorption and thermally treating with formaldehyde vapor, during which $H_2PtCl_6{\cdot}6H_2O$ adsorbed on the CFMs is reduced by the formaldehyde vapor and the formed Pt particles are deposited on the surface of fibers in CFMs. This procedure can not only synthesize Pt particles

* Corresponding authors. Tel.: +86 3517010699; fax: +86 3517016358.
E-mail address: han_gaoyis@sxu.edu.cn (G. Han).

0378-7753/$ – see front matter © 2011 Elsevier B.V. All rights reserved.
doi:10.1016/j.jpowsour.2011.05.060

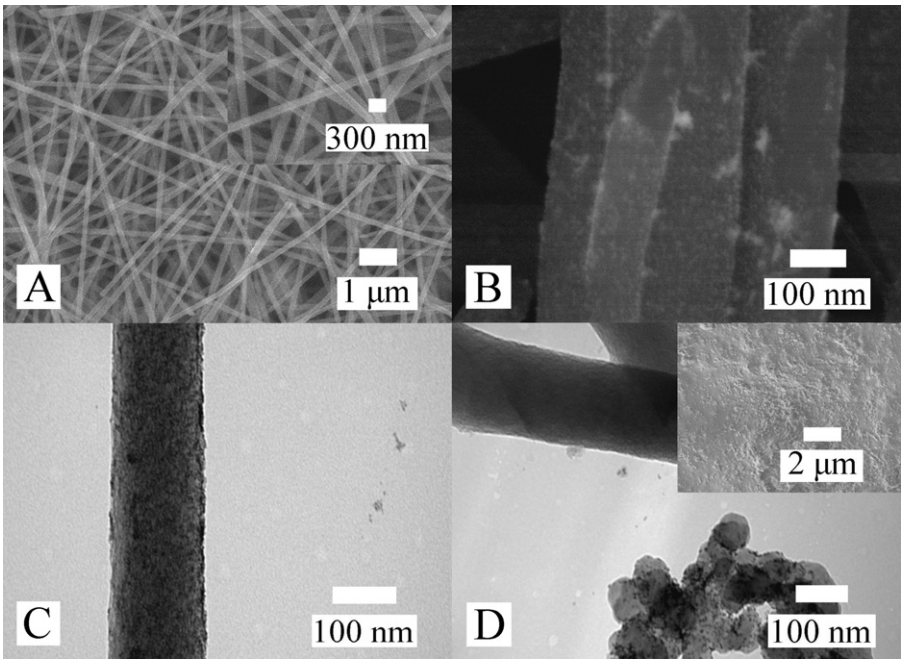

Fig. 1. SEM images of (A) CFMs and (B) as-prepared Pt-CFMs electrode (by combining the secondary electron image and the back-scattered electron image), (C) TEM images of the same electrode as (B), and (D) the TEM and SEM (inserted) images of as-prepared Pt/C-CFMs electrode.

with small size and homogeneous distribution on the surfaces of fibers directly, but also be solvent-saving and benign to the environment. It is expected that the obtained catalytic electrodes exhibit higher performance towards methanol electrooxidation.

2. Experimental

2.1. Chemicals and materials

Polyacrylonitrile and Nafion (5%) solution were obtained from Aldrich. The Pt/C (40 wt%) catalyst was obtained from Johnson Matthey Corp. All other chemicals employed in this paper were of analytical grade.

2.2. Apparatus

The micrographs of the samples were obtained by employing a scanning electron microscopy (SEM, JEOL-JSM-6701F) operating at an accelerating voltage of 10 kV and a transmission electron microscopy (TEM, JEM-1011) operating at the accelerating voltage of 80 kV, respectively. X-ray diffraction (XRD) patterns were recorded on a Bruker D8 Advance X-ray diffractometer (Cu Kα radiation). The content of Pt was determined by an IRIS Advantage inductively coupled plasma atomic emission spectroscopy system. The electrical conductivities were measured by using the four-point probe method. Electrochemical measurements were carried out on a CHI 660C electrochemistry workstation (Shanghai Chenhua, China) at 25 °C. Electrochemical impedance spectroscopy (EIS) was carried out at different potentials with an amplitude of 5 mV in the frequency range of 100,000–0.1 Hz. The ZView-2 fitting program was used to analyze the impedance parameters. The CFMs loaded with Pt or commercial Pt/C catalyst, a Pt plate and a saturated calomel electrode (SCE) were used as working, counter and reference electrode, respectively. High-purity nitrogen was used to deaerate the solutions and maintained above the electrolyte during the measurements.

2.3. Fabrication of the catalytic electrodes

The CFMs were fabricated according to the previously reported method [23]. The resulted CFMs with a thickness of about 50 μm were cut into strips with the size of 10 mm × 2.0 mm and used as electrodes directly. The Pt particles were deposited on the CFMs by reducing $H_2PtCl_6{\cdot}6H_2O$ adsorbed on the CFMs with formaldehyde vapor at 160 °C for 3.0 h, and the obtained catalytic electrodes were denoted as Pt-CFMs. By comparison, the electrodes labeled as Pt/C-CFMs had been fabricated by transferring 5.5 μl of the ultrasonic-treated mixture of Pt/C catalyst (5.0 mg), water (1.25 ml) and Nafion solution (5%, 0.25 ml) onto the CFMs, and the solvent was then evaporated at the room temperature. The contents of Pt on all the electrodes were kept about 0.183 mg cm^{-2}, and the geometric surface area of the electrodes immerged in the electrolyte was guaranteed to be about 0.04 cm^2.

3. Results and discussion

3.1. The characterization of CFMs, Pt-CFMs and Pt/C-CFMs

From the typical SEM image of the prepared CFMs shown in Fig. 1A, it can be found clearly that CFMs are formed by long fibers with smooth surface and relatively uniform diameter of about 150 nm. There are a large number of gaps in the mats, which is beneficial to disperse catalysts and diffuse reactants [10]. It is found that Pt nanoparticles are dispersed on the surface of the carbon fibers uniformly from the SEM image of Pt-CFMs electrode (Fig. 1B), and that the average diameter of Pt particles is approximately 5.0 nm from the TEM image of Pt-CFMs shown in Fig. 1C. However, the surface of CFMs is coated with Pt/C particles uniformly and the gaps dispersed on the mat have disappeared according to the SEM image of Pt/C-CFMs (inserted in Fig. 1D), furthermore, it can be found that the contact between the carbon fibers and catalyst particles is loose from the TEM image (Fig. 1D). The electrical conductivity of Pt/C-CFMs is about 42 S cm^{-1} which is 16% smaller than that of Pt-CFMs.

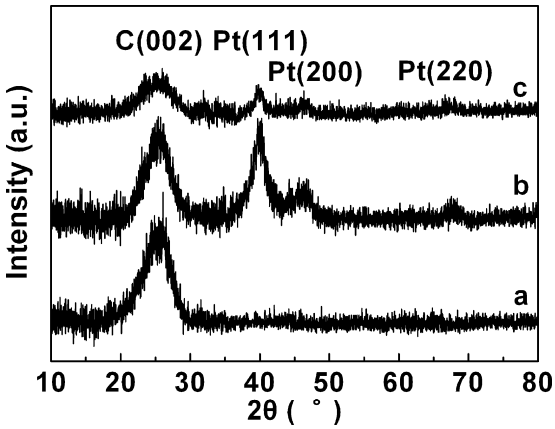

Fig. 2. XRD patterns of CFMs as-prepared (a), commercial Pt/C (b) and Pt-CFMs as-prepared (c).

The typical XRD patterns of the obtained electrodes are displayed in Fig. 2. It is clear that the as-prepared CFMs exhibit a broad diffraction peak at about 25.3° which is corresponding to the diffraction of (0 0 2) plane of the graphite carbon [1]. The diffraction peaks corresponding to Pt (1 1 1), (2 0 0) and (2 2 0) are located at about 39.9°, 46.3° and 67.7°, respectively. According to the Scherrer formula ($d = 0.89\lambda/B\cos\theta$), the average diameters of Pt particles are calculated based on the diffraction peak of Pt (1 1 1) and found to be about 5.0 and 3.7 nm in Pt-CFMs and commercial Pt/C, respectively.

3.2. Electrochemical properties of Pt-CFMs and Pt/C-CFMs electrodes

Cyclic voltammetry (CV) curve for CFMs shows no significant redox activity (Fig. 3A-a) in the aqueous solutions of 0.5 mol L^{-1} H_2SO_4 + 1.0 mol L^{-1} CH_3OH. However, the anodic current density on Pt-CFMs electrode in the positively going scan (I_f) increases with the increase of the scan potential, and reaches the maximum of about 81.4 mA cm^{-2} (445 mA mg^{-1} Pt) at 0.72 V which is significantly higher than 35.6 mA cm^{-2} (194 mA mg^{-1} Pt) at 0.67 V on

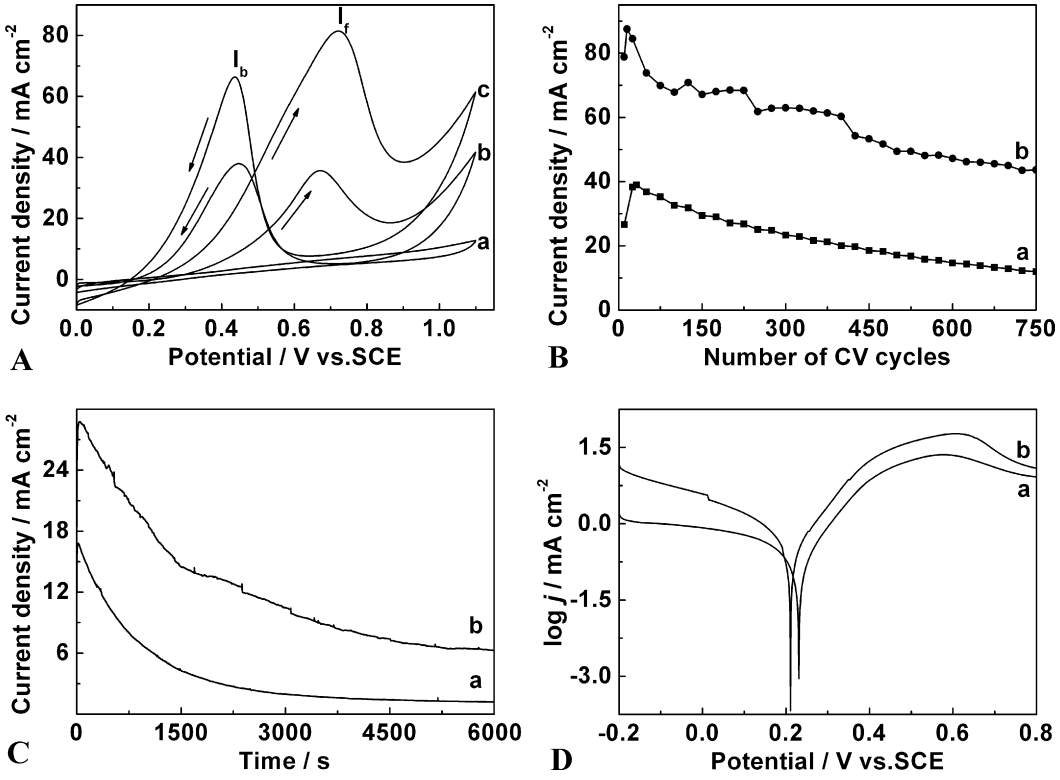

Fig. 3. (A) CV curves for methanol oxidation on (a) CFMs, (b) Pt/C-CFMs and (c) Pt-CFMs electrodes at a scan rate of 50 mV s^{-1}; (B) the plots of anodic peak current densities of methanol oxidation on (a) Pt/C-CFMs and (b) Pt-CFMs electrodes versus cycle numbers of CV at a scan rate of 100 mV s^{-1}; (C) chronoamperometric curves of methanol oxidation on (a) Pt/C-CFMs and (b) Pt-CFMs at a constant potential of 0.45 V (versus SCE); (D) the Tafel plots for methanol oxidation on the Pt/C-CFMs (a) and Pt-CFMs (b) at a scan rate of 1.0 mV s^{-1}. The electrolyte is 0.5 mol L^{-1} H_2SO_4 + 1.0 mol L^{-1} CH_3OH aqueous solution.

Pt/C-CFMs electrode. In the reverse scan, the other anodic peak (I_b) appears on both Pt-CFMs and Pt/C-CFMs electrodes, which may be attributed to the removal of the incompletely oxidized carbonaceous species formed in the positively going potential scan. The value of I_f/I_b is 1.23 on Pt-CFMs electrode which is higher than that on Pt/C-CFMs electrode (0.94), indicating that more intermediate carbonaceous species are oxidized to carbon dioxide in the positively going scan on Pt-CFMs electrode [24,25].

The diffusion coefficients for methanol on the electrodes of Pt-CFMs and Pt/C-CFMs are calculated based on the CV curves according to the following equation (Randles–Sevcik) [26]:

$$I_p = 0.4463nFAC\left(\frac{nFvD}{RT}\right)^{0.5} \quad (1)$$

where I_p is the peak current density (mA cm^{-2}), n the number of electrons that are involved in the redox reaction, F the Faraday constant (96,485 C mol^{-1}), A the surface area of the electrode (cm^2), C the concentration of methanol, v the scan rate, R the ideal gas constant, T the temperature (K), and D the diffusion coefficient of methanol (cm^2 s^{-1}). The diffusion coefficients of methanol are calculated to be about 5.31×10^{-6} cm^2 s^{-1} and 1.02×10^{-6} cm^2 s^{-1} on Pt-CFMs and Pt/C-CFMs electrodes, respectively, which shows that the rate of methanol diffusion in the catalytic layer of Pt-CFMs is higher than that of Pt/C-CFMs because of the high porosity in the Pt-CFMs electrode.

The anodic peak current densities for methanol oxidation on Pt-CFMs and Pt/C-CFMs electrodes during a total of 750 cycles in 0.5 mol L^{-1} H_2SO_4 + 1.0 mol L^{-1} CH_3OH are shown in Fig. 3B. It is found that the anodic peak current density in the positively going scan increases at initial cycles until it attains the maximum value and afterwards displays a downward trend with the successive CV scans for both the electrodes, for example, the peak current density approaches a maximum of about 87.5 mA cm^{-2} at the 15th cycle and then decreases to about 43.6 mA cm^{-2} at the 750th cycle, with a total decrease of 50.2% on Pt-CFMs electrode. However, the peak current density reaches its maximum of about 39.0 mA cm^{-2} at the 32nd cycle on Pt/C-CFMs electrode and then decreases to about 12.0 mA cm^{-2} at the 750th cycle, with a total decrease of 69.2%. The loss of the peak current density may result from: (1) the consumption of CH_3OH in the electrolyte during the CV scans, and (2) the poisoning and structural change of Pt catalysts, in which, the latter usually leads to the decrement of the peak current density and perturbation of the potentials during the CV scans in aqueous solutions especially in the presence of the organic compound. The above results indicate that the Pt-CFMs electrodes exhibit better long-term stability than Pt/C-CFMs electrodes.

From the plots of the polarized current density for methanol oxidation versus time shown in Fig. 3C, it can be found clearly that the current densities of methanol oxidation on both Pt-CFMs and Pt/C-CFMs electrodes present continuous decay with the increment of time after reaching their maximums. The current densities decrease to about 18.9 mA cm^{-2} and 6.5 mA cm^{-2} on Pt-CFMs and Pt/C-CFMs electrodes after a polarization time of 1000s, respectively. Furthermore, the decay of the current density on Pt-CFMs electrode exhibits a more gently decreasing trend, for example, there are 6.3 mA cm^{-2} and 1.2 mA cm^{-2} current densities retained on Pt-CFMs and Pt/C-CFMs electrodes after a polarization time of 6000s, respectively. It is clear that the reserved current density on the Pt-CFMs electrode is higher than that on the Pt/C-CFMs electrode, which accords with the results shown in Fig. 3A and B and denotes a strong electrocatalytic behavior towards methanol oxidation.

The exchange current densities (j_0) for methanol oxidation are also calculated based on the Tafel curves shown in Fig. 3D according to the equation [22,27]:

$$\eta = a + b\log j$$

$$a = -\frac{2.303RT}{\beta nF}\log j_0, \qquad b = \frac{2.303RT}{\beta nF} \quad (2)$$

where η is named as the over potential and β is the anodic charge transfer coefficient. According to the relationship between η and log$j$, the values of j_0 are calculated and found to be about 235.7 μA cm^{-2} and 174.7 μA cm^{-2} on electrodes of Pt-CFMs and Pt/C-CFMs, respectively. The j_0 value on Pt-CFMs electrode is about 1.35 times as large as that on Pt/C-CFMs electrode. And the Tafel slope is measured to be approximately 92.4 mV dec^{-1} for methanol oxidation on Pt-CFMs electrode compared with the slope of 99.1 mV dec^{-1} on Pt/C-CFMs electrode, which also indicates that Pt-CFMs electrodes exhibit higher catalytic ability for methanol oxidation.

The results obtained in this paper are different from which held generally that the small Pt particles exhibit higher exchange current density than large particles. Such factors as the following must be considered to clarify it: (1) it is unavoidable that a significant portion of Pt/C particles is detached from the substrate and isolated from the electrical circuit even with the most advanced electrodes prepared by wetting-drying method, resulting in a low Pt utilization, (2) the necessary addition of Nafion for proton transport tends to isolate carbon particles from each other in the catalyst layer, leading to poor electron transport [5,25], (3) the exchange current density measured by the method of quasi-steady state polarization and the catalytic activity towards methanol oxidation depend on the Pt catalyst particles in the circuit. So the Pt/C particles loaded on the substrate by wetting-drying process exhibit a small exchange current density and low catalytic activity to methanol oxidation because of the above-mentioned reasons.

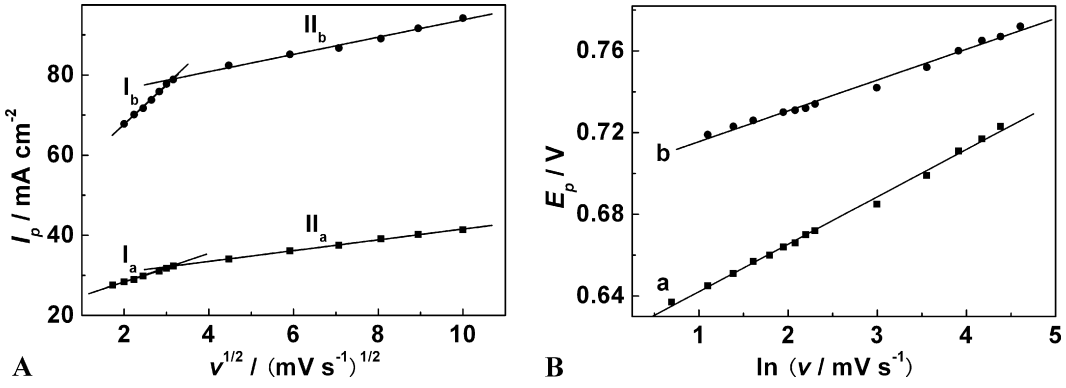

Fig. 4. (A) The plots of peak current densities versus square root of sweep rates (lines I_a and II_a for Pt/C-CFMs electrode; lines I_b and II_b for Pt-CFMs electrode) and (B) E_p versus ln(v) at different electrodes of (a) Pt/C-CFMs and (b) Pt-CFMs in 0.5 mol L^{-1} H_2SO_4 + 2.0 mol L^{-1} CH_3OH.

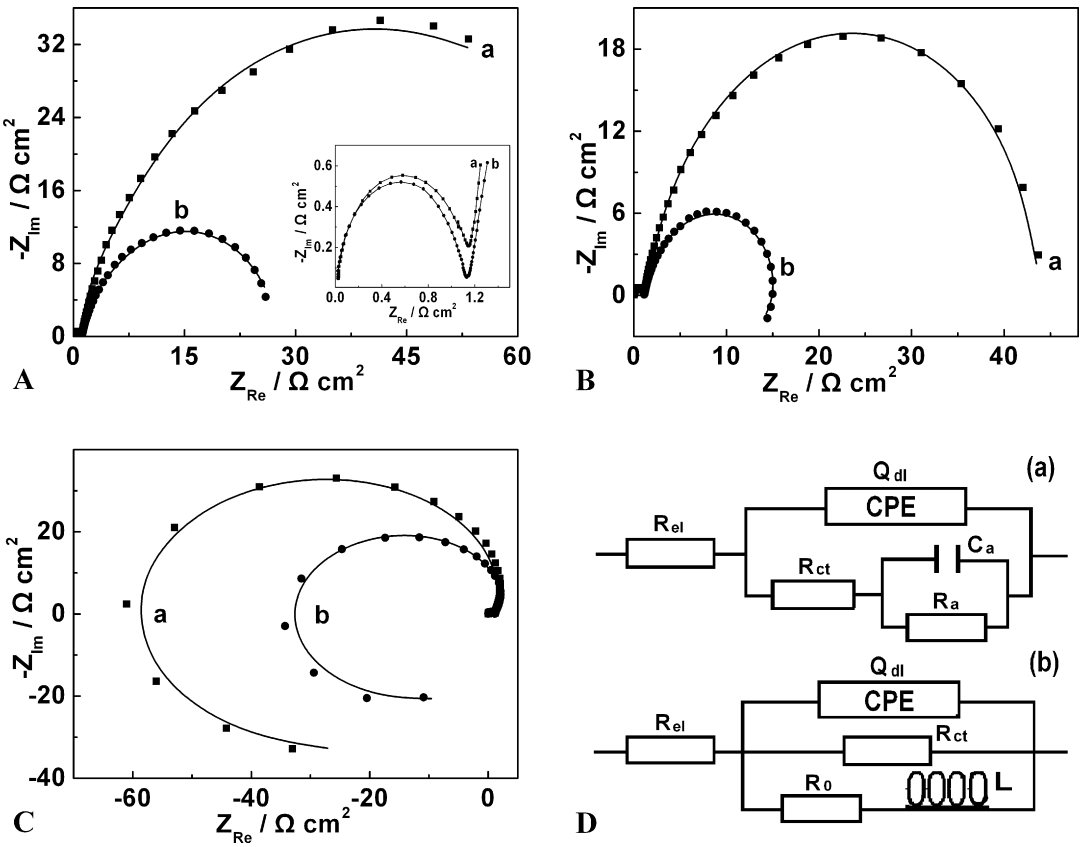

Fig. 5. Complex plane plots of the impedance of the Pt/C-CFMs (a) and Pt-CFMs (b) electrodes in 0.5 mol L^{-1} H_2SO_4 + 1.0 mol L^{-1} CH_3OH at various potentials of (A) 0.32 V, (B) 0.4 V, and (C) 0.50 V versus SCE, respectively. The lines represent the fits of the data to the equivalent circuit shown in (D) for methanol electrooxidation, (A and C) fit to D-a and (B) to D-b.

In order to obtain more information about methanol oxidation on Pt-CFMs and Pt/C-CFMs electrodes, the relationships between the anodic peak current density (I_p) and peak potential (E_p) obtained from the positively going CV scan versus different sweeping rates (v) have been studied and shown in Fig. 4. It is found clearly that there is a linear relationship between I_p and $v^{1/2}$ for methanol oxidation on Pt-CFMs and Pt/C-CFMs electrodes (Fig. 4A), and that the similar results are also observed when the electrolyte contains more methanol (see supplementary material), implying that the methanol oxidation on the catalytic electrodes is controlled by the diffusion process of methanol [8,28]. Additionally, it can be observed that the slopes of lines at smaller scan rates (I_a and I_b) are larger than that at larger scan rates (II_a and II_b) for both the electrodes, and that the slope of line I_b for Pt-CFMs electrode is 9.8 which is 3 times as large as that of line I_a for Pt/C-CFMs electrode (3.3), and the slope of line II_b for Pt-CFMs electrode is 2.2 which is 1.5 times as large as that of line II_a for Pt-CFMs electrode (1.3). This result reveals that the diffusion of reactive reagents in Pt-CFMs electrode is easier than that in Pt/C-CFMs electrode, which is consistent with the diffusion coefficients of methanol from CV data. The dependences of the peak potential (E_p) for methanol oxidation upon the ln(v) on the electrodes are shown in Fig. 4B, from which it can be found that the values of E_p for the methanol oxidation on Pt-CFMs and Pt/C-CFMs electrodes change positively when v increases, and that the linear relationship between E_p and ln(v) can be also observed obviously, indicating that the oxidation of methanol is an irreversible electrode process. It can be deduced that the Pt-CFMs electrodes have higher electrocatalytic behavior towards methanol oxidation than Pt/C-CFMs electrodes from the above-mentioned results and the fact that the slope of the line for methanol oxidation on Pt-CFMs electrodes (0.015) is smaller than that on Pt/C-CFMs electrodes (0.023).

The measurements of EIS are carried out in order to get the charge transfer resistance (R_{ct}) and evaluate the charge transfer property of methanol oxidation on the Pt-CFMs and Pt/C-CFMs electrodes [29]. From the complex plots of the EIS shown in Fig. 5, it can be found that all the complex plots consist of two semicircles or arcs in which the small ones at the high frequency are independent of potentials and may be associated with the electric double layer effect, whereas the large ones at low frequency appear to vary with potentials and may associate with R_{ct} which is related to the kinetics of the charge transfer reaction, furthermore, the semicircles in the low frequency for Pt-CFMs electrodes show smaller diameter than that for Pt/C-CFMs electrodes. The complex plots recorded at 0.32 V (Fig. 5A) show the capacitive behaviors and signify a reaction with one adsorbed intermediate, so the assumption that the rate-determining step is the dehydrogenation of methanol should be reasonable. The data of the plots in Fig. 5A can be simulated through the equivalent circuit shown in Fig. 5D-a. At about 0.40 V, the impedance data plotted in the complex plane for Pt-CFMs electrodes extend into the fourth quadrant while that for Pt/C-CFMs electrodes almost intersect with the real axes, which are featured by an inductive loop in low frequency for both electrodes because of the inductive behavior, indicating that the rate-determining step for methanol oxidation may be in a transition region [30]. The values of R_{ct} obtained from the EIS are about 16.1 and 39.4 Ω cm^2 for methanol oxidation on Pt-CFMs and Pt/C-CFMs electrodes, respectively, therefore it is proved that much faster charge transfer rates occur on Pt-CFMs during methanol electrooxidation. When the potential increases to 0.5 V,

the semicircles in low frequency flip over to the second quadrant and part of real component of the impedance becomes negative (Fig. 5C), and the data can also be simulated by using the equivalent circuit shown in Fig. 5D-a. This means that the R_{ct} becomes negative, which results from the passivation of the electrode surface and that the rate-determining step is the oxidation and removal of CO_{ads} [29,30].

The performance of Pt-CFMs electrode is superior to that of commercial Pt/C loaded on the CFMs although the size of Pt particles on the CFMs is larger than that of the commercial Pt/C catalyst. A conclusion can be drawn that the high performance of Pt-CFMs comes mainly from the relatively high conductivity of the carbon fibers and the close contact between Pt particles and carbon fibers, which make the Pt catalyst exhibit high utilization efficiency. It is expected that the Pt-CFMs electrodes can be developed as applicable electrocatalytic electrodes with superior performance.

4. Conclusions

The electrodes of Pt-CFMs with high performance have been constructed by combining the process of physical adsorption and the thermal treating with formaldehyde vapor. The most important advantage of this approach is economical and benign to the environment; besides, it is easy to obtain Pt nanoparticles with well-defined morphology and even distribution on the carbon fibers in CFMs. The investigative results reveal that the Pt particles supported on the carbon fibers in CFMs exhibit higher performance towards methanol electrooxidation. The process in which formaldehyde vapor is used as the reducer can be developed as a new means for preparation of noble metallic catalysts.

Acknowledgments

The authors thank the National Natural Science Foundation of China (21073115, 20604014) and Shanxi Province (2007021008), the Program for New Century Excellent Talents in University (NCET-10-0926) of China and the Program for the Top Young and Middle-aged Innovative Talents of Higher Learning Institutions of Shanxi Province (TYMIT and TYAL).

Appendix A. Supplementary data

Supplementary data associated with this article can be found, in the online version, at doi:10.1016/j.jpowsour.2011.05.060.

References

[1] Z. Lin, L.W. Ji, W.E. Krause, X.W. Zhang, J. Power sources 195 (2010) 5520.
[2] Y.Y. Mu, H.P. Liang, J.S. Hu, L. Jiang, L.J. Wan, J. Phys. Chem. B 109 (2005) 22212.
[3] S.Y. Wang, X. Wang, S.P. Jiang, Langmuir 24 (2008) 10505.
[4] H.S. Liu, C.J. Song, L. Zhang, J.J. Zhang, H.J. Wang, D.P. Wilkinson, J. Power Sources 155 (2006) 95.
[5] C. Wang, M. Waje, X. Wang, J.M. Tang, R.C. Haddon, Y.S. Yan, Nano Lett. 4 (2004) 345.
[6] G. Wu, L. Li, J.H. Li, B.Q. Xu, J. Power sources 155 (2006) 118.
[7] M. Tsuji, M. Kubokawa, R. Yano, N. Miyamae, T. Tsuji, M.S. Jun, S. Hong, S. Lim, S.H. Yoon, I. Mochida, Langmuir 23 (2007) 387.
[8] M.W. Xu, G.Y. Gao, W.J. Zhou, K.F. Zhang, H.L. Li, J. Power sources 175 (2008) 217.
[9] S.H. Liu, W.Y. Yu, C.H. Chen, A.Y. Lo, B.J. Hwang, S.H. Chien, S.B. Liu, Chem. Mater. 20 (2008) 1622.
[10] Z.H. Hou, F.Y. Zeng, B.H. He, W. Tao, C.Y. Ge, Y.F. Kuang, J.H. Zeng, Mater. Lett. 65 (2011) 897.
[11] S.H. Joo, C. Pak, D.J. You, S.A. Lee, H.I. Lee, J.M. Kim, H. Chang, D. Seung, Electrochim. Acta 52 (2006) 1618.
[12] H.X. Huang, S.X. Chen, C.E. Yuan, J. Power Sources 175 (2008) 166.
[13] F.B. Su, C.K. Poh, Z.Q. Tian, G.W. Xu, G.Y. Koh, Z. Wang, Z.L. Liu, J.Y. Lin, Energy Fuels 24 (2010) 3727.
[14] L.F. Dong, R.R.S. Gari, Z. Li, M.M. Craig, S.F. Hou, Carbon 48 (2010) 781.
[15] S. Basri, S.K. Kamarudin, W.R.W. Daud, Z. Yaakub, Int. J. Hydrogen Energy 35 (2010) 7957.
[16] A. Halder, S. Sharma, M.S. Hegde, N. Ravishankar, J. Phys. Chem. C 113 (2009) 1466.
[17] C. Kim, K.S. Yang, M. Kojima, K. Yoshida, Y.J. Kim, Y.A. Kim, M. Endo, Adv. Funct. Mater. 16 (2006) 2393.
[18] C. Kim, K.S. Yang, Appl. Phys. Lett. 83 (2003) 1216.
[19] G.Y. Han, B. Guo, L.W. Zhang, B.S. Yang, Adv. Mater. 18 (2006) 1709.
[20] W.X. Zhang, Y.Z. Wang, C.F. Sun, J. Polym. Res. 14 (2007) 467.
[21] C.S. Kong, T.H. Lee, S.H. Lee, H.S. Kim, J. Mater. Sci. 42 (2007) 8106.
[22] B. Guo, S.Z. Zhao, G.Y. Han, L.W. Zhang, Electrochim. Acta 53 (2008) 5174.
[23] M.Y. Li, G.Y. Han, B.S. Yang, Electrochem. Commun. 10 (2008) 880.
[24] G.Y. Zhao, C.L. Xu, D.J. Guo, H. Li, H.L. Li, J. Power Sources 162 (2006) 492.
[25] X.M. Liu, M.Y. Li, G.Y. Han, J.H. Dong, Electrochim. Acta 55 (2010) 2983.
[26] H. Gharibi, K. Kakaei, M. Zhiani, J. Phys. Chem. C 114 (2010) 5233.
[27] M.Y. Li, S.Z. Zhao, G.Y. Han, B.S. Yang, J. Power Sources 191 (2009) 351.
[28] H. Tang, J.H. Chen, Z.P. Huang, D.Z. Wang, Z.F. Ren, L.H. Nie, Y.F. Kuang, S.Z. Yao, Carbon 42 (2004) 191.
[29] E.H. Yu, K. Scott, R.W. Reeve, J. Electroanal. Chem. 547 (2003) 17.
[30] G. Wu, L. Li, B.Q. Xu, Electrochim. Acta 50 (2004) 1.